Current Research in Biotechnology 3 (2021) 308–316

Contents lists available at ScienceDirect

Current Research in Biotechnology

journal homepage: www.elsevier.com/locate/crbiot

On-spot biosensing device for organophosphate pesticide residue detection in fruits and vegetables

Subhankar Mukherjee [a], Souvik Pal [a,*], Prasenjit Paria [b], Soumyadeb Bhattacharyya [a], Koustuv Ghosh [a], Abhra Pal [a], Devdulal Ghosh [a], Om Krishan Singh [f], Priyabrata Sarkar [c], Bijay Kumar Behera [b], Shyamal Chandra Sukla Das [e], Sunil Bhand [d], Nabarun Bhattacharyya [a]

[a] Agri and Environmental Electronics (AEE) Group, Centre for Development of Advanced Computing (C-DAC), Sector – V, Salt Lake, Kolkata, West Bengal 700091, India
[b] Central Inland Fisheries Research Institute, Kolkata Monirampur, Barrackpore, Kolkata, West Bengal 700120, India
[c] Calcutta Institute of Technology. NH6, Banitabla, Uluberia, Howrah, West Bengal 711316, India
[d] Biosensor Lab. Department of Chemistry, BITS, Pilani –KK Birla Goa Campus, Goa 403726, India
[e] Regional Centre, ICAR-Central Inland Fisheries Research Institute, HOUSEFED Complex, Dispur, Guwahati 781 006, Assam
[f] Indian Institute of Technology, IITH Main Road, Near NH-65, Sangareddy, Kandi, Telangana 502285, Hyderabad

ARTICLE INFO

Keywords:
Enzyme
Biosensor
Organophosphate hydrolase
Pesticides
Imaging array
Fruits and vegetables

ABSTRACT

Acetylcholinesterase (AChE), a widely used enzyme for inhibition-based biosensors in pesticide residues detection, lags due to multiple-step operation, time-consuming incubation and reactivation/regeneration steps. Herein, this endeavour reports the development of Organophosphate Hydrolase (OPH), which has functional superiority over the AChE and explored in on-spot biosensing device for organophosphate pesticide residue detection in fruits and vegetables. The organophosphate degrading enzyme OPH is expressed from the '*opd*' gene through biotechnological tools. The OPH exhibited its best activity at pH 8.0 and subsequently thermal inactivation over 37 °C. The activity of the purified OPH enzyme was found 2.75 U mL^{-1} at λ_{max} 410 nm. Furthermore, the developed OPH is integrated into 96 well plate format with our previously reported $UIIS^{Scan}$ 1.1, an advanced imaging array technology based field-portable high-throughput sensory system. The developed biosensor revealed a linear range from 100 ng mL^{-1} to 0.1 ng mL^{-1} for detection of organophosphate pesticide residues with a negative slope i.e. y = 235.678x (ng mL^{-1}) – 62.8725 with R^2 = 0.99991 and n = 23. Moreover, the applicability of the developed biosensor was tested for market available fruits and vegetables. This is the first-ever reported OPH mediated on-spot biosensing device for pesticide residue detection in fruits and vegetables to the best of our knowledge.

Introduction

On-spot detection of organophosphate pesticide residues (OPs) has drawn tremendous attention as the technological progress in the contemporary sensor-based detection techniques. Several exploratory studies have already been completed on a different point of care rapid on spot detection. Among those, biosensor-based practices have emerged vigorously in the recent decade. Scientists have worked effortlessly to develop optical and electrochemical bio-sensory techniques for a minute amount of OP detection in water and food products (Arjmand et al., 2017; Gai et al., 2018; Mahmoudi et al., 2019; Sahub et al., 2018; Uniyal and Sharma 2018). In some recent works, synthetic nanomaterials are also being highlighted in the sensor development towards pesticide detection. MnO_2 nanozyme mediated electrochemical assay for OPs (Wu et al., 2021), pH-sensitive Quantum Dots (QDs) mediated fluorimetric detection of OPs (Yang et al., 2021), QD-functionalized electropolymerized photoelectrochemical sensor towards OPs detection (Wang et al., 2019), GeO_2 nanozymes mimicking peroxidase-like activity for colorimetric pesticide assay (Liang and Han 2020b), Gold nanoparticle aggregation-induced fluorescence quenching technique for OPs detection (Liang and Han 2020a) are among the most significant scientific outputs in this domain. Towards the development of biosensors against OPs, acetylcholinesterase (AChE) is the abundantly explored bio-receptor (Table 1). These reported pieces of literature exploited the well-known property of inhibiting AChE by OPs. These OPs are well known for inhibiting the Acetylcholinesterase (AChE) enzyme causing synaptic cholinergic crisis through the accumulation of acetylcholine and

* Corresponding authors.
E-mail addresses: souvipal@gmail.com, p2010814g@alumni.bits-pilani.ac.in (S. Pal), beherabk18@yahoo.co.in (B.K. Behera).

https://doi.org/10.1016/j.crbiot.2021.11.002
Received 17 August 2021; Revised 9 November 2021; Accepted 11 November 2021

2590-2628/© 2021 The Author(s). Published by Elsevier B.V.
This is an open access article under the CC BY-NC-ND license (http://creativecommons.org/licenses/by-nc-nd/4.0/).

Table 1
Comparison of sensing technique with earlier reported biosensors.

Pesticide detected	Principle & procedure	Linear range	LOD	Operation time	Instrument Field portability	Reference
Paraoxon, Dichlorvos, Malathion and Triazophos	AChE on glutathione quantum dot-based optical transduction	10 ng L^{-1} − 500 ng L^{-1}	Paraoxon (1.62×10^{-15} M), Dichlorvos (75.3×10^{-15} M), Malathion (0.23×10^{-9} M) and Triazophos (10.6×10^{-12} M)	>24 hrs	Not Field portable	(Korram et al., 2020)
Paraoxon	AChE immobilised biopolymeric electrospun fibrous mats based optical transduction	10–60 ppb	10 ppb	20 min	Not Field portable	(Cacciotti et al., 2020)
Phoxim, carbaryl	AChE inhibition based optical transduction	Phoxim (0.1–10 mg L^{-1}), carbaryl (0.05–5 mg L^{-1})	Phoxim (0.39 mg L^{-1}), carbaryl (0.25 mg L^{-1})	22 min	Not Field portable	(Jin et al., 2020)
OPs	AChE immobilized nano-interface based electrochemical transduction	0.01–100 nM	0.01 nM	>10 min	Not Field portable	(Singh et al., 2020)
Chlorpyrifos	AChE immobilized nanocomposite based electrochemical transduction	0.02 nM to 20000 nM	0.02 nM	>10 min	Not Field portable	(Liu et al., 2020)
Triazophos	AChE inhibition based optical transduction	0 to 117 nM	4.69 nM	>1.5 hrs	Not Field portable	(Qing et al., 2020)
Paraoxon	AChE film biosensor on graphene oxide/polyimide flexible electrode based electrochemical transduction	0.005–0.150 μg mL^{-1}	0.0014 μg mL^{-1}	–	Not Field portable	(Jia et al., 2020)
Propoxur	AChE inhibition based electrochemical transduction	5.5×10^{-15}–1.0×10^{-4} mol L^{-1}	$(2.89 \pm 0.97) \times 10^{-17}$ mol L^{-1}	>1 hr	Not Field portable	(Juárez-Gómez et al., 2020)
OPs	AChE on Boron doped polycrystalline diamant based electrochemical transduction	2 to 6 nM	–	26 min	Not Field portable	(Khaldi et al., 2020)
OPs like Monocrotophos	AChE inhibition based optical transduction	20 ng mL^{-1} to 0.1 ng mL^{-1}	0.1 ng mL^{-1}	30 min	Field portable	(Mukherjee et al., 2019)
OPs	OPH on micro well plate based optical transduction	100 ng mL^{-1} to 0.1 ng mL^{-1}	0.1 ng mL^{-1}	10 min	Field portable	This work

continued stimulation of acetylcholine receptors (Hsieh et al., 2001). AChE is known to terminate the cholinergic nerve impulses in synapses by breaking down acetylcholine through hydrolysis. The enzyme being a serine protease, contains a serine esteratic domain in its active site. The active site includes a few negative ionic charges to interact with cationic substrates and inhibitors. The AChE forms a reversible enzyme-substrate complex and promotes hydrolysis of the substrate through subsequent acetylation and deacetylation. In this context, Organophosphate pesticides (OPs), being substrate analogues, are involved in the irreversible inhibition of AChE (Tougu 2001). The AChE does not show OPs hydrolysis. Owing to this reason, OPs detection using AChE involves indirect OPs sensing through enzymatic inhibition of AChE through OPs.

However, these inhibition-based biosensors lag due to multiple-step operation, such as time-consuming incubation and reactivation/regeneration steps (Mulchandani et al., 2001a). Therefore, replacing AChE with another bioreceptor that can rapidly sense OPs with advantages over the discussed drawbacks of the inhibition-based biosensors is of paramount importance.

In this context, Organophosphorus hydrolase (OPH) is the most critical OP-degrading enzyme encoded from the '*opd*' gene by many soil bacteria (Singh 2009). OPH is a metalloprotein (~35 kDa) containing divalent Zn^{2+} at its catalytic centre. Like other amidohydrolase superfamily proteins, OPH has a TIM barrel-fold (Bigley and Raushel 2013; Parthasarathy et al., 2016). Several bacterial species like *Agrobacterium radiobacter*, *Pseudomonas diminuta MG*, *Flavobacterium* sp. ATCC 27,551 by origin contains OPH encoding gene '*opd*' in their dissimilar plasmid. The presence of '*opd*'-gene has was reported in different other bacterial species, too. OPH can catalyse the hydrolysis of many OPs pesticides containing bonds like P—F, P—O, P—S, and P—CN (Reeves et al., 2008; Wales and Reeves 2012). It has specificity towards OP pesticides, viz., diazinon, parathion, methyl parathion, paraoxon, coumaphos, dursban, sarin, soman. Thus, the presence of OPs can be detected using OPH as a biological receptor and converting the enzymatic reaction to a measurable signal in a biosensor. In the enzymatic hydrolysis of OPs by the OPH enzyme, two protons and an alcohol moiety are generated, showing chromophoric or electroactive nature. This property provides enormous OPH applicability in various sensors ranging from enzymatic inhibition-based biosensors to fluorometric, electrochemical, and pH-based sensors (Bian et al., 2022).

We have recently demonstrated a field-portable high-throughput sensory system, UIIS^{Scan}1.1, an advanced imaging array technology based field-portable high-throughput sensory system (Mukherjee et al., 2019). Herein, we report the synthesis of the OPH enzyme from scratch by exploiting the '*opd*' gene retrieved from NCBI-Gene Bank. Furthermore, the complete protein-coding sequence (CDS) was amplified using the polymerase chain reaction (PCR) protocol. The PCR amplified '*opd*' gene is cloned, taking *E. coli* as a host to produce the OPH enzyme. Moreover, the hydrolysis activity of OPH was enhanced by expressing a diverse set of '*opd*' gene variants from different bacteria. Finally, the expressed OPH coupled 96 micro-well plate format was integrated with UIIS^{Scan} 1.1 as an on-spot, power independent biosensing system to detect OP residues in fruits and vegetables. As a result, the instrument offers better efficacy and applicability over the other reported literature (Table 1).

Materials and methods

Materials and instrumentation

Magnesium chloride ($MgCl_2$), 10X PCR buffer, deoxyribonucleotide triphosphate (dNTP) and Pfu polymerase were purchased from Sigma-Aldrich (USA). pET28a (+) expression vector, nickel-charged affinity resin (Ni-NTA) column were purchased from Invitrogen. Magnesium chloride, coomassie brilliant blue R-250 (CBB) were procured from Sigma-Aldrich (USA). Recombinant protein A agarose kit was purchased from Invitrogen. Organophosphate (OP) Pesticide Mix (containing Carbophenothion, Ethion, Malathion, Parathion; 100 μg mL^{-1} each component in hexane), Organophosphorus Pesticides Mix A (containing Azinphos-methyl, Chlorpyrifos, Dichlorvos, Disulfoton, Ethoprophos, Fenchlorphos, Parathion-methyl, Prothiofos; 2000 μg mL^{-1} each component in hexane: acetone (9:1)), 2-(Cyclohex ylamino)ethanesulfonic acid (CHES) were procured from Sigma-Aldrich India.

Retrieval of nucleotide sequence

The complete sequence of organophosphorus hydrolase was retrieved from NCBI of *Flavobacterium sp*. (AY766084.1). The downloaded sequence was used for conserved domain and superfamily analyses using NCBI CD-search tools (NCBI, Conserved Domain search. https://www.ncbi.nlm.nih.gov/Structure/cdd/wrpsb.cgi., 2020).

Invitro gene synthesis

OPH gene was synthesised following the protocol described by Hoover and Lubkowski (2002) with some modifications (Hoover and Lubkowski 2002). The OPH gene sequence was divided into twelve (12) oligonucleotides of 60 nucleotides (nt) each segment, with 10 nt overlaps region at both the 5′ and 3′ ends between adjoining oligonucleotides. The oligonucleotides were synthesised at the 50 nmol scale with desalt purification. Equal volumes of each oligo (25 μM each) were combined and mixed. The mixture was diluted to a final concentration of 0.2 ng mL^{-1} of each oligonucleotide. The PCR reaction mixture comprised 2.5 μL of 10X PCR buffer, 2 mM $MgCl_2$, 0.2 mM each dNTP and 2.5 U of Pfu polymerase where 'U' represents the enzyme unit and is expressed as μmol/min. The PCR program consisted of a denaturation step cycle at the PCR program involving one denaturation step at 94 °C for 5 min followed by 35 cycles at 94 °C for 30 s, 55 °C for 30 s, 72 °C for 2 min and a final incubation cycle at 72 °C for 15 min.

Gene amplification

An aliquot of the gene assembly mixture (5 μL) was diluted 10-fold in 50 μL of PCR mixture. The reaction mixture comprised 5 μL of 10X PCR buffer, 2 mM $MgCl_2$, 0.2 mM each dNTP and 2.5 U of pfu polymerase and the two outermost primers at 10 pmol each. The PCR program consisted of one cycle of denaturation step at 94 °C for 60 s, followed by 25 cycles at 94 °C for 45 s, 68 °C for 45 s, 72 °C for 5 min and a final extension at 72 °C for 10 min. In addition, the amplified product was purified using a PCR purification kit purchased from Qiagen.

Cloning and transformation

The synthesised gene fragments were then purified and cloned in cloning vector pEASY-blunt vector at NdeI/XhoII sites. The probable clones were screened by restriction digestion, and the nucleotide sequence of OPH gene was confirmed by sequencing. The gene was then ligated into a cloning vector. The 10 μL of ligation reaction mixture was mixed with 100 μL of DH5α competent cells and incubated at 4 °C for 30 min, after completion of incubation, heat shock was given at 42 °C for 45 s. Further, the tubes were quickly transferred on ice for 2 min, and finally, the volume made up to 1 mL with sterile Luria broth. Then, the tubes were placed at 37 °C for 1 hr in a shaking incubator. After incubation, 100 μL of bacterial culture plated on AXI plate containing 100 μL ampicillin (Initial concentration: 100 mg mL^{-1}), 120 μL X-gal (Initial concentration: 100 mg mL^{-1}), 24 μL IPTG (Initial concentration: 1 M) and the plates were incubated overnight at 37 °C.

The plasmid from positive isolates was screened by restriction digestion, and the gene was amplified using primers complementary to sequences in the vector backbone, flanking the synthetic gene. The amplified products (gene of interest) were sequenced in forward and reverse directions. After sequence verification, the insert was subcloned into pET28a (+) expression vector at NdeI/XhoI sites and transformed into *E. coli* BL21 competent cells to generate recombinant proteins.

Protein extraction and purification

A single positive colony was inoculated into the sterile broth. The culture was grown till optical density 260 nm ($OD_{600\ nm}$) 0.6 and induced with 1 mM IPTG at 37 °C for overnight. The culture was pelleted down, and the pellet was washed twice with 1X PBS. After washing, the pellet was resuspended in 1X PBS and sonicated four times at 30 MHz for the 30 s in ice-cold conditions. The homogenates were further centrifuged at 12000 rpm for 15 min at 4 °C, and the supernatant was collected. One part of the supernatant was passing through the Ni-NTA column and eluted with different concentrations of Imidazole.

Protein quantification and SDS-PAGE analysis

Protein concentration of supernatant, flow-through and purified fractions were determined by Bradford method (Bradford 1976), using BSA as the standard. All the samples were then immediately subjected to gel electrophoresis. The soluble bacterial proteins from the supernatant flow through were separated by 1-D SDS-PAGE composed of 12 % (W/V) resolving gel with a 5 % (W/V) stacking gel at a constant potential of 200 V on a mini-Protean 3-electrophoresis cell purchased from Bio-Rad (Laemmli 1970). Protein molecular weight markers (58445, Bio-rad) were co-run with the samples. Protein bands were visualised in the gel after staining with CBB.

MALDI TOF MS/MS analysis

In-gel digestion was performed after removal of Coomassie-stained. The gel pieces were reduced with 5 mM TCEP and further alkylated with 50 mM iodoacetamide digestion. Finally, the proteins were digested with 1 μg trypsin for 16 hr at 37 °C. The resulting peptides were extracted with acetonitrile containing 0.1 % TFA (Shevchenko et al., 2006) and dried by a rotary evaporator. The dried peptides pellet was dissolved in 5 μL of TA buffer (0.1 % TFA in 100 % Acetonitrile). The peptides obtained were mixed with HCCA (α-Cyano-4-hydroxycinnamic acid) matrix (5 mg mL^{-1} α-Cyano- 4-hydroxycinnamic acid in 1:2 ratio of 0.1 % TFA and 100 % ACN) in 1:1 ratio, and the resulting 2 μL was spotted onto the MALDI plate [(MTP 384 ground steel (Bruker Daltonics, Germany)]. After air-drying the sample, it was analyzed on the MALDI TOF/TOF ULTRAFLEX III instrument (Bruker Daltonics, Germany). External calibration was done with standard peptide (PEPMIX Mixture) supplied by Bruker, with masses ranging from 1046 to 3147 Da. Further investigations were done with Flex analysis software (Version 3.3) in reflectron ion mode with an average of 500 laser shots at mass detection range between 500 and 5000 *m/z* for obtaining the MS-MS. The masses obtained in the MS-MS were submitted for Mascot search in the "Bacteria" database to identify the protein.

Immunisation of rabbit and purification anti-OPH antibody

Rabbits were immunised subcutaneously. The 0.5 mg of purified protein with Complete Freund's Adjuvant (CFA) was administered for the primary immunisation. First booster immunisation, 0.25 mg of protein with Freund's Incomplete Adjuvant (IFA), was administered after 14 days of the primary immunisation. A second booster immunisation was carried with 0.25 mg of protein in IFA after 28 days of the first booster immunisation. Then, final immunisation was carried with 0.25 mg of protein in IFA after 49 days of the second booster immunisations. Blood was collected 5 days after the final immunisation, and antibody was purified from serum using protein A IgG Purification Kit (Thermo, 44667) to estimate the antibody titer. Titre was estimated using indirect ELISA (enzyme-linked immunosorbent assay) with different dilutions (1:2000, 1:4000, 1:8000, 1:16000 and 1:32000) in 0.5 % BSA fraction.

Further, a large amount of IgG antibody has been purified from serum using a recombinant protein A Agarose kit (Thermo 20365). First, a 5 mg antibody was dissolved in equal volumes of the resin bed and packed the column. Next, the column pack was equilibrated by adding 5 mL of the binding buffer and allowing the solution to drain through the column. Next, the serum was diluted with binding buffer (1:1) and added to the column. Next, the column was washed with 15 mL of the binding buffer. Finally, the bound antibody was eluted with 5 mL of elution buffer. Immediately after elution, the pH of the eluted fractions is adjusted to physiologic pH with neutralization buffer.

Purification OPH protein by affinity chromatography

Anti–OHP antibody to be coupled was dialysed in 10 mM carbonate buffer, pH 11. A total of 5 mg antibody was dissolved in equal volumes of the resin bed. The bottle of resin was equilibrated to room temperature before opening. The washed resin and the antibody solution (5 mg of protein per mL of resin) was combined. The excess coupling buffer was removed from the reaction slurry. The 50 mM Tris buffer (pH 11) was added to the resin and incubated for 2 hr to quench and block non-reacted 1,1 ´-carbonyl diimidazole (CDI) groups. The tris quenching buffer was drained, and the resin was washed with phosphate PBS-buffer and the finally obtained coupled resin was packed into a column.

Enzymatic assay

The activity of the OPH enzyme was measured using a UV–Vis spectrophotometer (Make Biotek, Model Epoch 2) by monitoring the production of p-nitrophenol (pNP). The standard assay reactions used 0.1 mL of purified OPH solution mixed with 2.9 mL of 50 mM sodium phosphate buffers (pH 8.0) containing 0.1 mL of 10 mM methyl parathion (as substrate) for incubation for 10 min at 37 °C. The activity was assayed by measuring the formation of p-nitrophenol at 410 nm. The OPH activity was calculated following the equation:

$$\text{Units/mL enzyme} = \frac{\left[\{(A_{410nm})/min\}_{Test} - \{(A_{410nm}/min\}_{Blank}\right](3)(df)}{(18.3)(0.1)}$$

Where,

3 = Volume (in mL) of assay;

df = Dilution factor;

0.1 = Volume (in mL);

18.3 = Millimolar extinction coefficient of pNP at 410 nm of enzyme used.

Unit definition: One unit hydrolyses 1.0 μmol OPs per minute at pH 8.0 at 37 °C.

Uniform illumination imaging system (UIIS) and biosensing principle

The UIIS system was fabricated using market available scanning device (FUJITSU fi-65F). The flatbed type scanner (W × D × H ~ 40.64 × 233.68 × 144.78 in mm) is integrated as an advanced colour Contact Image Sensor (CIS) with a USB interface 2.0. The system has the efficiency to produce images at 600 dpi. The instrument can be operated at a dynamic temperature and relative humidity range of 5 °C to 35 °C and 20 % − 80 %, respectively

Fig. 1. Photograph of UIIS prototype.

(Fig. 1). The UIIS has a provision to accommodate OPH integrated 96 well-plate format that slides in the middle of the acquisition bed of the device. The initial images were captured in 24-bit BMP, which further converted into Mahanalobis distance using basic R, G, and B raw data extracted from the images. MATLAB R2019a and Microsoft Visual C++ 6.0 standard edition were explored towards raw data capture, analysis and graphical user interface display. The detailed fabrication and data algorithm development were reported elsewhere (Mukherjee et al., 2019).

Due to broad substrate specificity and the ability to hydrolyse phosphorous-oxygen bond, phosphorous-cyanide bond, phosphorous-fluorine and phosphorous-sulfur bond, OPH was considered for detection OPs. During the interaction with OPH and OPs, two protons and one alcohol, which are often electroactive or chromophoric, are generated (Mulchandani et al., 2001b; Theriot and Grunden 2011). Thus, by optimising the reaction parameters, OPs can be quantified optically in terms of the production of pNP (Jain et al., 2019) (Supplementary figure SF1). The resultant yellow colour of the produced pNP was recorded simultaneously with UV–Visible spectrophotometer and the developed UIIS based system.

Preparation of field-collected fruits and vegetable samples

Raw fruits and vegetables were procured from the local market as samples. The extraction of pesticide residues from samples were optimised based on the reported literature (Fenik et al., 2011). The best-optimised composition was found in a mixture of water, 1 mM NaCl, Acetonitrile with a ratio of 90:8:2. Further, the preparation of field-collected samples for the biosensing experiment was carried out using the optimised mixture of solvents. The samples were soaked into the solvent mixture for 25 min. Finally, the supernatant was collected for further experiments.

Results and discussion

Choice of bioreceptor

Organophosphate hydrolase is an amidohydrolase enzyme and can hydrolyse a broad list of most toxic organophosphate pesticides containing P—F, P—O, P—S, and P—CN bonds (Theriot and Grunden 2011). The OPH performs a nucleophilic attack on the phosphorus centre of different OPs, thus catalyses the hydrolysis process.

OPH cannot hydrolyse the non-organophosphate pesticides like organochlorines which lack nucleophilic attack centre phosphorus and the aforementioned P—F, P—O, P—S, and P—CN bonds in their chemical structure. However, the same type of reaction mechanism, i.e. hydrolysis, can be applied towards sensor development against those non-organophosphate pesticides, but we have to change the hydrolysing enzyme. Some hydrolysing evidence of organochlorine pesticides has been mentioned elsewhere (Singh et al., 2017).

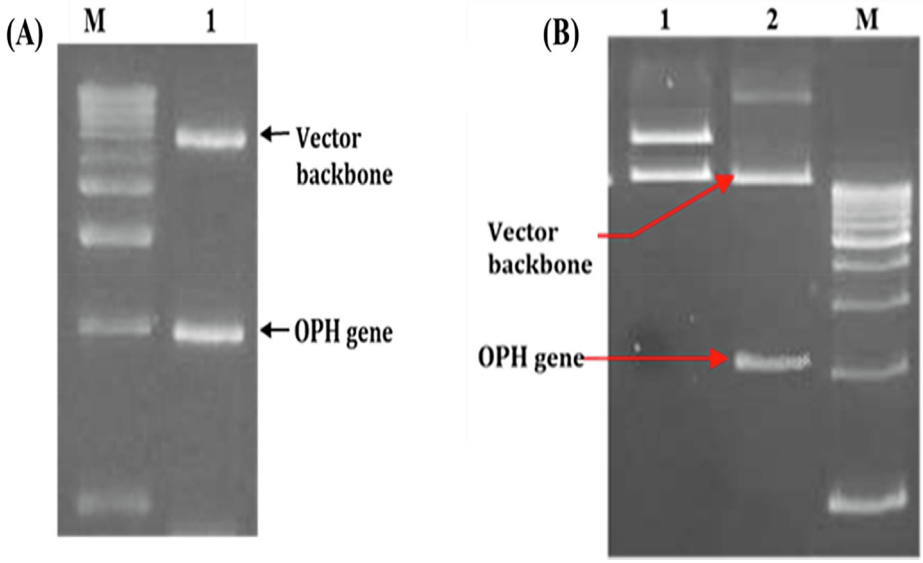

Fig. 2. (A) Gel electrophoresis of OPH gene clone to pEASY vector. Lane M; 500 bp DNA ladder marker. Lane 1 restriction digestion of OPH gene cloned in pEASY + where plasmid of ~2.9 kb and the gene of ~927 bp have been observed; **(B)** Gel electrophoresis of OPH gene clone to pET28a vector. Lane 1 uncut pET28a vector and OPH gene clone to pET28a. Lane 2 restriction digestion of OPH gene cloned in pET28a Lane M; 500 bp DNA ladder marker.

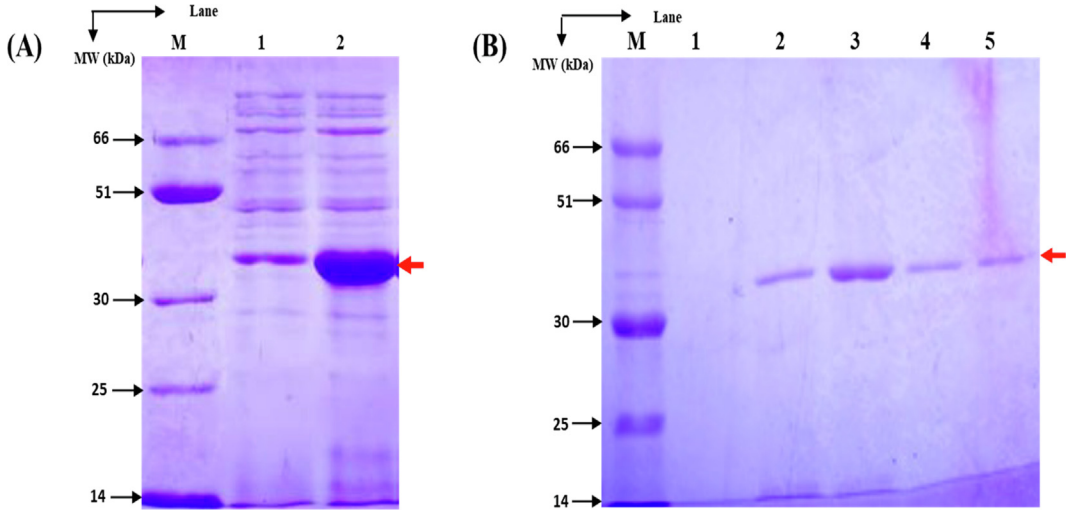

Fig. 3. (A) 12% SDS-PAGE profile of express proteins in E. coli. (Lane 1) whole cell extract before induction; (Lane 2) whole cell extract 16 h after induction. Red colour arrows indicating expressed proteins. **(B)** 12% SDS-PAGE profile after purification of express proteins in E. coli by using by Ni-NTA column. (Lane 1) eluted in 100 mM; (Lane 2) 250 mM Immidazole; (Lane 3) 500 mM Immidazole; (Lane 4) 750 mM Immidazole; (Lane 5) 1 M Immidazole. Red colour arrows indicating expressed proteins. (For interpretation of the references to colour in this figure legend, the reader is referred to the web version of this article.)

Retrieve of nucleotide sequence

The complete sequence of OPH from *Flavobacterium* sp. was retrieved from NCBI GenBank and further characterised with NCBI-CD search tools. Protein domains were initially described as the most stable or autonomously folding units of protein structure. Conserved Domains Database (CDD) of NCBI annotates protein sequences with conserved domain footprints and functional sites inferred from these footprints.

In vitro gene synthesis, cloning and transformation

The gene encoding OPH was designed to maximise expression in *E. coli*. Thus, 972 base pairs gene encoding OPH was synthesised by recursive PCR and cloned into pEASY-blunt vector at NdeI/XhoII. The sequence of the insert was checked by sequencing. The presence of insert was confirmed by NdeI/XhoII digestion (Fig. 2 (A)).

Subsequent cloning of the Oph gene into the pET28a (+) vector resulted the pET-Oph gene recombinant plasmid (Fig. 2 (B)). Finally, the vector was cloned into *E. coli* cell and subjected to the expression of recombinant protein. The expression of protein depends on optimal induction temperature, IPTG concentration, and induction time for the expression of recombinant OPH protein. The maximum yield of soluble protein OPH was achieved at an incubation temperature of 30 ° C, IPTG concentration of 0.2 mM, and incubation time for 6 hrs.

Protein purification and SDS-PAGE analysis

The 1D profile revealed that a band with a molecular weight of 35 kDa was highly expressed after induction with 1 mM IPTG (Fig. 3 (A)). CCB-stained 12 % SDS-polyacrylamide gels separated the protein into 16 bands in the molecular weight range of 14 to > 100 kDa (kDa). The electrophoretic profiles showed that a band with a molecular weight of 35 kDa was highly expressed after induction with 1 mM IPTG. Further, the expressed protein was purified by running the whole-cell extract through the Ni-NTA column and eluted with different concentrations of imidazole. The purified protein observed with SDS-PAGE showed that most of the proteins were eluted at 500 mM imidazole (Fig. 3 (B)).

MALDI TOF MS/MS analysis

The protein band was excised, digested with trypsin for Matrix-assisted laser desorption/ionisation-mass spectrometry (MALDI-TOF-MS). The peptide mass fingerprint profiles generated from this band were used in a database search. The peptide fragments produced were used to search against the SwissProt database and taxonomy set to Bacteria (*Eubacteria*) using the MASCOT search program. The presence of OPH protein was identified.

Enzymatic activity assay

The enzymatic activity of purified OPH was determined by mixing methyl parathion with OPH at 37 °C and pH 8.0. As a result, OPH converted methyl parathion into p-nitrophenol (Supplementary Figure SF2). The concentration of pNP was measured using a UV–Visible spectrophotometer at 410 nm at a different time interval. The OPH activity was found to be 2.75 U mL^{-1}.

Optimisation of ionic strength and pH

The effects of different ionic strength and pH of CHES on the activity of the OPH enzyme was studied. The enzyme activity was measured with various ionic strengths (10, 50, 100, 150 and 200 mM CHES) and pH (6.5–10) for methyl parathion as substrate and incubated for 10 min at 37 °C. The results are presented in Supplementary Figure SF3 by measuring the formation of pNP at 410 nm.

The result clearly showed that with the increase in the ionic strength of CHES, the response signal gradually increased up to 150 mM, and then decreased (Supplementary Figure SF3). Thus, further experiments were carried out with 150 mM CHES. It is also clear from Supplementary Figure SF4 that OPH exhibited maximum activity at pH 8.0.

Optimisation of temperature

The temperature plays an essential role in enzyme activity. Therefore, the optimal temperature for enzyme activity was determined by measuring the enzyme activity at different temperatures in the range of 25 °C to 50 °C. The optimum temperature was determined and presented as Supplementary Figure SF5. Enzymes exhibited the greatest

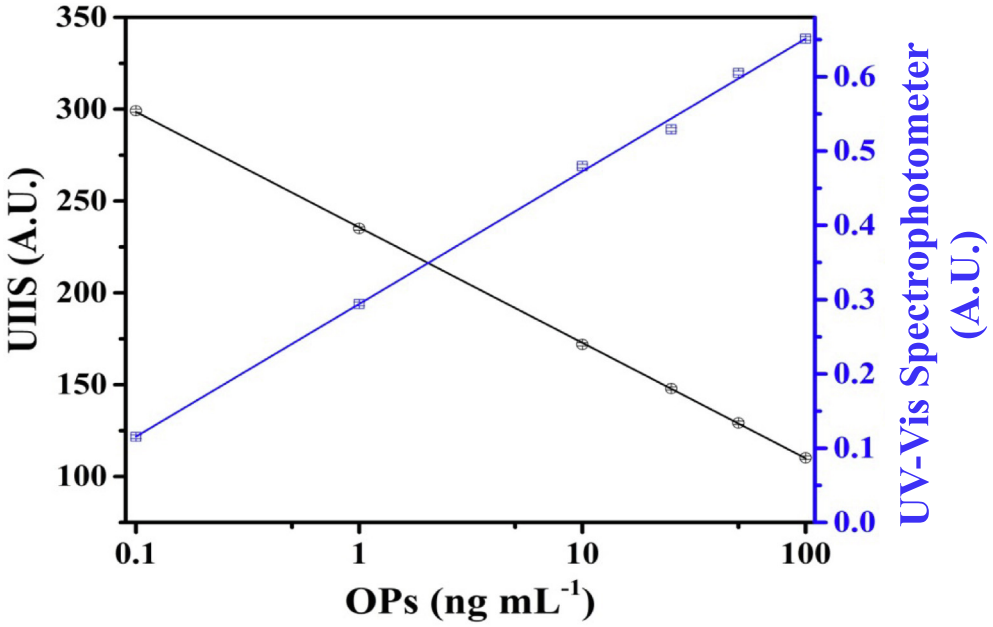

Fig. 4. Calibration curve for OPs using UIIS^{Scan}1.1 and multiplate reader data.

Table 2
Recovery studies using unknown pesticide samples.

[OPs] added ng mL^{-1}	Developed Device		
	[OPs] found (ng mL^{-1}) Mean ± S.D.	R.E. (%)	Recovery (%)
50	51.26952 ± 0.55	−2.53904	102.53904
10	10.42016 ± 0.17	−4.2016	104.2016
1	0.95786 ± 0.014	4.214	95.786

change in signal intensity at 30 °C. The system lost activity in the temperature range 40–50 °C. The residual activity was 10.5 % for enzymes at the temperature 50 °C. Above temperature 37 °C, the enzyme activity significantly decreased due to the thermal inactivation.

Standard curve and system calibration

As focused on OPs, the certified pesticide spiked samples were prepared in water, NaCl, and Acetonitrile mixture as described earlier. The resultant colour was recorded simultaneously with a UV–Visible spectrophotometer and the developed UIIS based system. As OPs act as a substrate for OPH enzymes, thus the colour intensity was continuously increasing with increasing concentrations of OPs. The maximum signal intensity was stabilised within 5 min, after which the signal intensity tended to a stable value, indicating the saturated binding interaction with active target groups in the enzyme. The developed yellow colour of the product pNP is read out using a UV–Visible spectrophotometer at 410 nm. This experiment produces a positive slope while plotting the concentrations of OPs against OD. The same reaction is replicated in the developed UIIS device. In this case, with the increase in the colour intensity, the Mahanalobis distance value decreases.

Moreover, the data plot exhibits a negative slope while plotting the concentrations of OPs against Mahanalobis distance values (represented as index). Although the nature of the plots is different using UIIS and conventional UV–Visible spectrophotometer, both instruments are very much correlated in nature. The data obtained using a spectrophotometer for a higher concentration of OPs were found non-linear due to limitations in the Beer-Lambert Law, which has not been observed in the UIIS system. Further, these data were used to plot the graph for the UIIS prototype.

The standard calibration curve was plotted for parallel experimentations, i.e., spectrophotometer and a developed UIIS system Fig. 4. The obtained data from the plate reader and UIIS system based measurement exhibited the linear range from 100 ng mL^{-1} to 0.1 ng mL^{-1} with a limit of detection (LOD) 0.1 ng mL^{-1}. The linear equation for spectrophotometer was found to be y = 0.17858 + 0.294x (ng mL^{-1}) (R^2 = 0.99809, n = 23). In contrast, the equation for the UIIS system was found with a negative slope, i.e. y = 235.678x (ng mL^{-1}) – 62.8725 with R^2 = 0.99991 and n = 23 (where, 'y' is the measured OD and colour index for spectrophotometer and UIIS system respectively, 'x' is the measured pesticide concentration, '$R^{2\prime}$ is the goodness of fit measure for linear regression model and 'n' is the number of observations).

The obtained correlation coefficients of both methods reveal high similarity in results. Based on a Tukey pairwise comparison, developed prototype (p = 0.17 ± 0.03) was not significantly different compared to the Spectrophotometer (p = 0.11 ± 0.03) at the 95 % confidence interval. The correlation coefficients (r) are 0.999834 and 0.99896853 from the data graph and theoretical calculation. To determine the characteristics of the instrument in terms of sensitivity, response time, or LOD with significant differences (p less than 0.05), analysis of variance (ANOVA model 1) and Tukey tests were performed. Randomised experiments based on the obtained data were designed with at least three replications. The statistical significance between the developed prototype and spectrophotometer is found to be less than 0.05. There are no significant differences amongst the instruments while comparing ANOVA and Tukey pairwise test.

Recovery and field-collected sample analysis

Recovery experiments were conducted to evaluate the accuracy and precision of the developed UIIS biosensor. Known amounts of OPs were used to spike fruit and vegetable samples. Recovery experiments were performed OPs fortified at levels of 50, 10 and 1 ng mL^{-1}; the recoveries of OPs were found in the range 95 to 104 % (Table 2).

Fig. 5. Preparation of field collected samples towards parallel analysis using developed UIIS system and LC-MS instrument.

Further, the unknown field samples exposed to OPs were exploited parallel to the developed UIIS biosensor and conventional liquid chromatography-mass spectrometry (LC-MS) technique to validate the system applicability. Total 54 samples were tested for three commodities, i.e. apple, eggplant and grapes. First, the market-collected samples were treated with washing solution: 0.01 M Tris Buffer – pH 8.00 containing 2.5 % Acetonitrile. Then samples were soaked in the washing solution for 1 hr. Finally, the extracted solution was filtered and divided into three batches for parallel measurement (Fig. 5).

Total 54 samples were marked as D1 to D54, tested with LC-MS. Obtained chromatogram of various samples for OPs analysis is mentioned in Supplementary Figure SF6-SF9. In addition, standard OPs samples were used for the preparation of the standard curve. Data obtained for standard OPs samples are mentioned in Supplementary Table ST3. Data obtained using LC-MS/MS for the standard samples were plotted to draw a standard calibration curve (Supplementary Figure SF10). The linear equation was obtained from the plot of pesticide concentrations against the peak area as $y = 897.98251 \times (\text{ng mL}^{-1})$. The samples were tested with a developed UIIS system. The image of test samples is depicted in Supplementary Figure SF11. Finally, the data received from the techniques, i.e. LC-MS and colorimetry based UIIS system, was compared, correlated, and the result was shown in Supplementary Table ST1. The data marked in red colour was quoted as 'No-Go', which signifies that both systems confirm the presence of pesticides. In contrast, the data marked in green colour refers to the conclusion that both the systems reveal the absence of pesticides, and thereby quoted as 'Go'. Comparing the data from the techniques, i.e. LC-MS and colorimetry based UIIS system, it was found that LC-MS exhibited 3.70 % samples above 1 ng mL^{-1} and 13 % samples below 1 ng mL^{-1} of OPs. In contrast, the colorimetric UIIS revealed 11 % samples above 1 ng mL^{-1} and 11 % below 1 ng mL^{-1} of OPs. UIIS data exhibited 90.74 % resemblance (Correlation coefficient (r) = 0.998877399) with LC-MS data.

Conclusion

This endeavour reports a unique technique of production of OPH that is further exploited in developing an on-spot OP residues detection device in fruits and vegetables. The evaluated optimum conditions yield OPH efficacy as a stable bio-recognition element over the other reported materials towards pesticide sensing. The activity of purified OPH enzyme was evaluated and further integrated with imaging array technology, i.e. contact image sensor (CIS). The developed prototype exhibited excellent correlation while comparing with UV–Vis Spectrophotometer. Moreover, the recovery studies provide the applicability of the fabricated prototype as a field-portable tool in environmental diagnostics. The system was tested for market available fruits and vegetable samples. In parallel validation with LC-MS/MS, the prototype has proven its vast applicability in agri setup, retail stores, and household uses with 90.74 % resemblance. To the best of our knowledge, this is the first report on developing an efficient, effective, and user-friendly device to measure pesticide residues in field-collected samples by integrating the OPH enzyme.

CRediT authorship contribution statement

Subhankar Mukherjee: Investigation, Methodology, Formal analysis, Data curation, Visualization, Writing – original draft. **Souvik Pal:** Investigation, Methodology, Validation, Writing – review & editing. **Prasenjit Paria:** Formal analysis, Data curation, Writing – original draft. **Soumyadeb Bhattacharyya:** Formal analysis, Writing – review & editing. **Koustuv Ghosh:** Formal analysis, Writing – review & editing. **Abhra Pal:** Software, Supervision, Validation. **Devdulal Ghosh:** Software, Supervision, Validation. **Om Krishan Singh:** Supervision, Project administration, Funding acquisition. **Priyabrata Sarkar:** Conceptualization, Project administration. **Bijay Kumar Behera:** Project administration, Funding acquisition. **Shyamal Chandra Sukla Das:** Conceptualization, Supervision, Validation. **Sunil Bhand:** Conceptualization, Project administration. **Nabarun Bhattacharyya:** Conceptualization, Project administration, Funding acquisition.

Declaration of Competing Interest

The authors declare that they have no known competing financial interests or personal relationships that could have appeared to influence the work reported in this paper.

Acknowledgement

Authors acknowledge the funding by Electronics System Development and Application Division (ESDA), Ministry of Electronics and Information Technology (MeitY), Government of India [Grant ID: 26

(4)/2019-ESDA, dated 23/01/2020] and ICAR-National Agricultural Science Fund (NASF) [Grant ID: NASF/MECH-8015/2019-20, dated: 29/02/2020]. The authors are also thankful to the Ministry of Electronics and Information Technology (MeitY), Government of India, for their continuous support.

Appendix A. Supplementary data

Supplementary data to this article can be found online at https://doi.org/10.1016/j.crbiot.2021.11.002.

References

Arjmand, M., Saghafifar, H., Alijanianzadeh, M., Soltanolkotabi, M., 2017. A sensitive tapered-fiber optic biosensor for the label-free detection of organophosphate pesticides. Sens. Actuators, B. 249, 523–532.

Bian, X., Chen, D., Han, L., 2022. Taking full advantage of the structure and multi-activities of mineralized microbial surface-displayed enzymes: Portable three-in-one organophosphate pesticides assay device. Chem. Eng. J. 429, 132317. https://doi.org/10.1016/j.cej.2021.132317.

Bigley, A.N., Raushel, F.M., 2013. Catalytic mechanisms for phosphotriesterases. Biochim. Biophys. Acta. Proteins. Proteom. 1834 (1), 443–453.

Bradford, M.M., 1976. A rapid and sensitive method for the quantitation of microgram quantities of protein utilizing the principle of protein-dye binding. Anal. Biochem. 72 (1-2), 248–254.

Cacciotti, I., Pallotto, F., Scognamiglio, V., Moscone, D., Arduini, F., 2020. Reusable optical multi-plate sensing system for pesticide detection by using electrospun membranes as smart support for acetylcholinesterase immobilisation. Mater. Sci. Eng. C. 111, 110744. https://doi.org/10.1016/j.msec.2020.110744.

Fenik, J., Tankiewicz, M., Biziuk, M., 2011. Properties and determination of pesticides in fruits and vegetables. Trends. Analyt. Chem. 30 (6), 814–826.

Gai, P., Zhang, S., Yu, W., Li, H., Li, F., 2018. Light-driven self-powered biosensor for ultrasensitive organophosphate pesticide detection via integration of the conjugated polymer-sensitized CdS and enzyme inhibition strategy. J. Mater. Chem. B. 6 (42), 6842–6847.

Hoover, D.M., Lubkowski, J., 2002. DNAWorks: an automated method for designing oligonucleotides for PCR-based gene synthesis. Nucleic acids research. 30, e43-e43.

Hsieh, B.H., Deng, J.F., Ger, J., Tsai, W.J., 2001. Acetylcholinesterase inhibition and the extrapyramidal syndrome: a review of the neurotoxicity of organophosphate. Neurotoxicology. 22 (4), 423–427.

Jain, M., Yadav, P., Joshi, A., Kodgire, P., 2019. Advances in detection of hazardous organophosphorus compounds using organophosphorus hydrolase based biosensors. Crit. Rev. Toxicol. 49 (5), 387–410.

Jia, L., Zhou, Y., Wu, K., Feng, Q., Wang, C., He, P., 2020. Acetylcholinesterase modified AuNPs-MoS_2-rGO/PI flexible film biosensor: Towards efficient fabrication and application in paraoxon detection. Bioelectrochemistry. 131, 107392. https://doi.org/10.1016/j.bioelechem.2019.107392.

Jin, L., Hao, Z., Zheng, Q., Chen, H., Zhu, L.i., Wang, C., Liu, X., Lu, C., 2020. A facile microfluidic paper-based analytical device for acetylcholinesterase inhibition assay utilizing organic solvent extraction in rapid detection of pesticide residues in food. Anal. Chim. Acta. 1100, 215–224.

Juárez-Gómez, J., Ramírez-Silva, M.T., Guzmán-Hernández, D., Romero-Romo, M., Palomar-Pardavé, M., 2020. Construction and optimization of a novel acetylcholine ion-selective electrode and its application for trace level determination of propoxur pesticide. J. Electrochem. Soc. 167 (8), 087501. https://doi.org/10.1149/1945-7111/ab8874.

Khaldi, K., Sam, S., Gabouze, N., 2020. Acetylcholinesterase modified porous silicon for electrochemical measurement of total active immobilized enzyme amount and effective malathion detection. I2M 19 (1), 51–57.

Korram, J., Dewangan, L., Karbhal, I., Nagwanshi, R., Vaishanav, S.K., Ghosh, K.K., Satnami, M.L., 2020. CdTe QD-based inhibition and reactivation assay of acetylcholinesterase for the detection of organophosphorus pesticides. RSC Adv. 10 (41), 24190–24202.

Laemmli, U.K., 1970. Cleavage of structural proteins during the assembly of the head of bacteriophage T4. Nature. 227 (5259), 680–685.

Liang, B.o., Han, L., 2020a. Displaying of acetylcholinesterase mutants on surface of yeast for ultra-trace fluorescence detection of organophosphate pesticides with gold nanoclusters. Biosens. Bioelectron. 148, 111825. https://doi.org/10.1016/j.bios.2019.111825.

Liang, X., Han, L., 2020b. White peroxidase-mimicking nanozymes: colorimetric pesticide assay without interferences of O_2 and color. Adv. Funct. Mater. 30 (28), 2001933. https://doi.org/10.1002/adfm.v30.2810.1002/adfm.202001933.

Liu, X., Sakthivel, R., Liu, W.-C., Huang, C.-W., Li, J., Xu, C., Wu, Y., Song, L., He, W., Chung, R.-J., 2020. Ultra-highly sensitive organophosphorus biosensor based on chitosan/tin disulfide and British housefly acetylcholinesterase. Food chem. 324, 126889. https://doi.org/10.1016/j.foodchem.2020.126889.

Mahmoudi, E., Fakhri, H., Hajian, A., Afkhami, A., Bagheri, H., 2019. High-performance electrochemical enzyme sensor for organophosphate pesticide detection using modified metal-organic framework sensing platforms. Bioelectrochemistry. 130, 107348. https://doi.org/10.1016/j.bioelechem.2019.107348.

Mukherjee, S., Pal, S., Pal, A., Ghosh, D., Sarkar, S., Bhand, S., Sarkar, P., Bhattacharyya, N., 2019. UIIS^{Scan}1.1: A Field portable high-throughput platform tool for biomedical and agricultural applications. J. Pharm. Biomed. Anal. 174, 70–80.

Mulchandani, A., Chen, W., Mulchandani, P., Wang, J., Rogers, K.R., 2001a. Biosensors for direct determination of organophosphate pesticides. Biosens. Bioelectron. 16 (4-5), 225–230.

Mulchandani, P., Chen, W., Mulchandani, A., Wang, J., Chen, L., 2001b. Amperometric microbial biosensor for direct determination of organophosphate pesticides using recombinant microorganism with surface expressed organophosphorus hydrolase. Biosens. Bioelectron. 16 (7-8), 433–437.

NCBI, Conserved Domain search. https://www.ncbi.nlm.nih.gov/Structure/cdd/wrpsb.cgi. 2020.

Parthasarathy, S., Parapatla, H., Nandavaram, A., Palmer, T., Siddavattam, D., 2016. Organophosphate hydrolase is a lipoprotein and interacts with Pi-specific transport system to facilitate growth of Brevundimonas diminuta using OP insecticide as source of phosphate. J. Biol. Chem. 291 (14), 7774–7785.

Qing, Z., Li, Y., Li, Y., Luo, G., Hu, J., Zou, Z., Lei, Y., Liu, J., Yang, R., 2020. Thiol-suppressed I_2-etching of AuNRs: acetylcholinesterase-mediated colorimetric detection of organophosphorus pesticides. Microchim. Acta. 187, 1–9.

Reeves, T.E., Wales, M.E., Grimsley, J.K., Li, P., Cerasoli, D.M., Wild, J.R., 2008. Balancing the stability and the catalytic specificities of OP hydrolases with enhanced V-agent activities. Protein Eng. Des. Sel. 21 (6), 405–412.

Sahub, C., Tuntulani, T., Nhujak, T., Tomapatanaget, B., 2018. Effective biosensor based on graphene quantum dots via enzymatic reaction for directly photoluminescence detection of organophosphate pesticide. Sens. Actuators, B. 258, 88–97.

Singh, A.P., Balayan, S., Hooda, V., Sarin, R.K., Chauhan, N., 2020. Nano-interface driven electrochemical sensor for pesticides detection based on the acetylcholinesterase enzyme inhibition. Int. J. Biol. Macromol. 164, 3943–3952.

Singh, B.K., 2009. Organophosphorus-degrading bacteria: ecology and industrial applications. Nat. Rev. Microbiol. 7 (2), 156–164.

Singh, S.P., Guha, S., Bose, P., Kunnikuruvan, S., 2017. Mechanism of the hydrolysis of endosulfan isomers. J. Phys. Chem. A. 121 (27), 5156–5163.

Theriot, C.M., Grunden, A.M., 2011. Hydrolysis of organophosphorus compounds by microbial enzymes. Applied Microbiology and Biotechnology. 89 (1), 35–43.

Tougu, V., 2001. Acetylcholinesterase: mechanism of catalysis and inhibition. Cent. Nerv. Syst. Agents. Med. Chem. 1, 155–170.

Uniyal, S., Sharma, R.K., 2018. Technological advancement in electrochemical biosensor based detection of organophosphate pesticide chlorpyrifos in the environment: A review of status and prospects. Biosens. Bioelectron. 116, 37–50.

Wales, M.E., Reeves, T.E., 2012. Organophosphorus hydrolase as an in vivo catalytic nerve agent bioscavenger. Drug Test. Anal. 4, 271–281.

Wang, J., Lv, W., Wu, J., Li, H., Li, F., 2019. Electropolymerization-induced positively charged phenothiazine polymer photoelectrode for highly sensitive photoelectrochemical biosensing. Anal. Chem. 91 (21), 13831–13837.

Wu, J., Yang, Q., Li, Q., Li, H., Li, F., 2021. Two-dimensional MnO_2 nanozyme-mediated homogeneous electrochemical detection of organophosphate pesticides without the interference of H_2O_2 and color. Anal. Chem. 93 (8), 4084–4091.

Yang, Q., Li, Q., Li, H., Li, F., 2021. pH-Response quantum Dots with orange–red emission for monitoring the residue, distribution, and variation of an organophosphorus pesticide in an agricultural crop. J. Agric. Food Chem. 69 (9), 2689–2696.